Stereoelectronic and Solvation Effects Determine Hydroxymethyl Conformational Preferences in Monosaccharides

Christopher B. Barnett and Kevin J. Naidoo*

Department of Chemistry, University of Cape Town, Rondebosch 7701, South Africa

Received: July 29, 2008; Revised Manuscript Received: September 11, 2008

Although the conformational preferences in glucose and galactose have been studied since the early 1970s, only recently have the glucose and galactose hydroxymethyl populations been resolved by combining $^3J_{HH}$ and $^2J_{HH}$ NMR coupling data using a modified Karplus equation. A preference for gauche conformations is observed in monosaccharides, but the reasons for this are not understood. We calculated the free energy of rotation profiles for glucose and galactose primary alcohols using a semiempirical description of the monosaccharides in QM/MM simulations. From this we observed excellent agreement between our simulated population distributions for glucose gg/gt/tg = 35:57:3 and galactose gg/gt/tg = 4:86:7 with those measured from NMR. A stereoelectronic analysis of the minimum energy conformations using natural bond orbitals provides a clear description of the stabilizing contribution to the gauche conformers stemming from the C−H bonding and the C−O antibonding orbital interactions, specifically $\sigma_{C6-H} \rightarrow \sigma^*_{C5-O5}$ and $\sigma_{C5-H} \rightarrow \sigma^*_{C6-O6}$. Analysis of the solution trajectories reveals that persistent intramolecular hydrogen bonds and intermolecular bridging hydrogen bonds formed by water molecules between the ring oxygen and the hydroxymethyl group further stabilizes the gt conformation making it the preferred rotamer in both hydrated glucose and galactose. The hydroxymethyl quantum mechanics/molecular mechanics molecular dynamics trajectories and derived rotational free energies for these monosaccharides in water solutions explain that the experimental observations are due to a combination of competing stereoelectronic (gauche), electronic (intramolecular hydrogen bonding), and electrostatic (solvent-saccharide hydrogen bonding) factors.

Introduction

Understanding and predicting macromolecular conformation is the first step in the structure function paradigm. While the conformational space of macromolecules is complex the primary rotors underlying the complexity are located in the monomers and dimers. The multiple bonding sites available from primary and secondary hydroxyls and the ring puckering in carbohydrates are the reasons for the great variety of conformational preferences observed for the same set of monomeric building blocks in oligosaccharides. This feature is routinely exploited in glycoproteins when an oligosaccharide provides a cell with its unique tag making cell−cell recognition possible (an important part of the immune response).

The flexibility and folding of oligosaccharides is due to their ability to rotate about the glycosidic linkages that join the monosaccharides. A linkage involving the hydroxymethyl group provides the most flexibility for oligosaccharides. The hydroxymethyl group (primary alcohol) has three staggered rotamers about the O5−C5−C6−O6 dihedral angle, ω (Figure 1) namely gauche−gauche (gg), gauche−trans (gt) and trans−gauche (tg). The first descriptor refers to the relation between the O5 and O6 atoms as given by the O5−C5−C6−O6 torsion. The second descriptor refers to the relation between the C4 and O6 atoms as given by the C4−C5−C6−O6 torsional angle. These rotamers are shown in Figure 1c,e,g for glucose and Figures 1d,f,h for galactose.

Experimental observation of the glucose (Figure 1a) hydroxymethyl group in aqueous solution reveals a preference for gauche conformers. However, the results obtained from ^{1}H NMR experiments are ambiguous about which gauche conformer is most prevalent in water since both the gg conformer[1,2] and the gt conformer[2] have been proposed as most favored. Furthermore, functionalization of saccharides affects the conformational preferences of the hydroxymethyl group.[3] When the OH functionality is changed at the C6 and C4 positions there is a reversal in the order of the ^{1}H NMR chemical shifts for the hydroxymethyl group pro-chiral hydrogens.[4] Galactose (Figure 1b) differs from glucose through the change of the hydroxyl on the C4 carbon from equatorial to axial but continues to display a gauche preference. However along with the positional change of the 4-hydroxyl group (OH4) the conformational preference changes from gt > gg > tg in glucose to gt > tg > gg in galactose.[1,2,5] NMR along with IR spectroscopy and optical rotation experiments[6] in a variety of solvents and intramolecular hydrogen bond motifs were inconclusive about the underlying reasons for the change in hydroxymethyl conformational populations resulting from the configurational change in the 4-hydroxyl group.

The contention about the rotameric preference ranking arises mostly from the form of the Karplus equation used in the analysis of $^2J_{HH}$ as this can have a dramatic effect on the population ratios predicted from an NMR experiment.[7] Combining $^3J_{HH}$ coupling data with $^2J_{HH}$ coupling results in an increase in accuracy for stereospatial assignments since $^3J_{HH}$ depends mainly on the C−C torsion angle (ω), while $^2J_{HH}$ couplings depend both on the C−C and C−O torsion angles.[2] Using the two $^3J_{HH}$ and $^2J_{HH}$ coupling data sets and a newly derived Karplus equations computed from density functional theory Stenutz et al. found that for glucose gt > gg > tg and for galactose gt > tg > gg.[2]

* To whom correspondence should be addressed. E-mail: Kevin.Naidoo@uct.ac.za. Fax: +27-21-686-4333.

10.1021/jp8067409 CCC: $40.75
Published on Web 11/06/2008

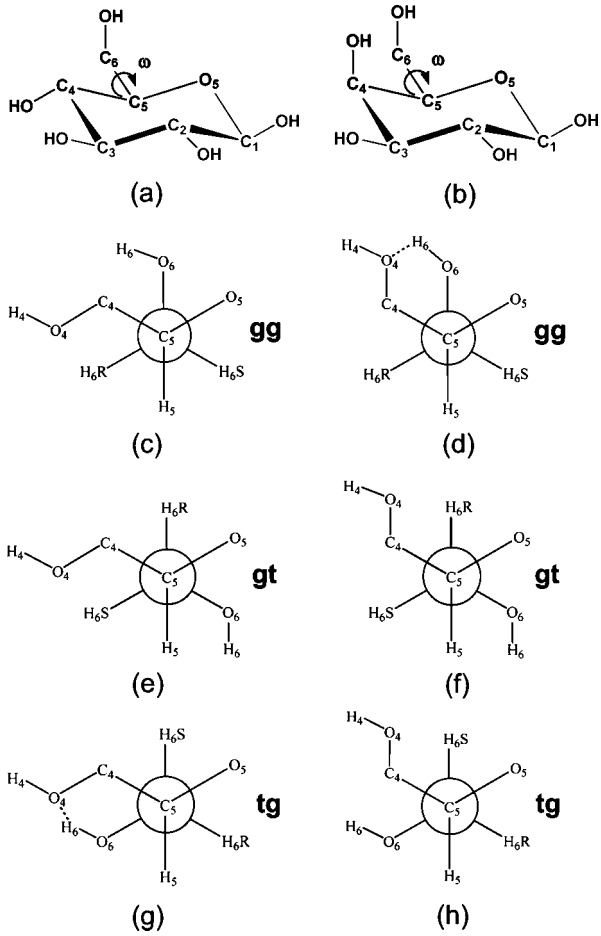

Figure 1. Definition of names for relevant atoms of (a) β-D-glucose and (b) β-D-galactose. Newman projections for (c) gg, (e) gt, and (g) tg conformers of glucose and (d) gg, (f) gt, and (h) tg of galactose.

NMR experiments revealed that the gg conformer population changed according to the solvent polarity leading to postulates that the gauche conformational preference may be the result of solvent effects.[8] Early computational studies probed the electronic[9] and solvent effects[10] on the hydroxymethyl preferences of glucopyranose. A semiempirical study of D-glucopyranose using continuum solvent models reported by Cramer and Truhlar[11] showed that only after solvent models were included did the relative hydroxymethyl ordering agree with experimental NMR values. They ascribed the unusual conformational preference of the primary alcohol in glucose to intramolecular hydrogen bonding induced by the solvent. Tvaroška's analysis[12] of a series of ab initio calculations on D-glycero-hexopyranosides supported the gg > gt > tg ordering where intramolecular hydrogen bonding was given as the reason for stabilizing the gg and gt conformers in particular a hydrogen bond between O5 and the 6-hydroxyl group. However, Duus and Bock[8] alluded to the existence of an intrinsic stereoelectronic effect being responsible for the gg, gt preference in Me-(α and β)-4-deoxy-D-glucose. In this compound no 1, 3 diaxial interactions destabilize the tg conformer yet gg and gt rotamers are still favored. More recently a high level ab initio (MP2/cc-pVTZ/IEFPCM//MP2/cc-pVTZ) free energy study of 5-(hydroxymethyl) tetrahydropyran using a continuum solvent concluded that rotamer populations and pathways are governed by a mixture of structural and stereoelectronic effects.[13]

The gauche effect has been argued to be the major stereoelectronic reason for this unusual preference in both monomers. This is the tendency for the adoption of gauche (synclinal) conformations as a result of a maximum number of gauche interactions between polar bonds about a torsional angle X−C−C−Y where the atoms X and Y are electronegative.[14] Using only this stereochemical reason as an explanation for the conformational preference seen in solution does not completely explain the gt, gg, and tg relative preferences; however, it is continually cited in the absence of a molecular understanding of the contributions of intramolecular hydrogen bonding, the solvent and its role in intermolecular hydrogen bonding.[11,12,15] Here we produce, from QM/MM adaptive umbrella sampling simulations of glucose and galactose in explicit solvent, complete hydroxymethyl rotational free energy surfaces with the intention of teasing out the roles of these competing effects that result in the unexpected conformational ordering.

Methods

Quantum Mechanics/Molecular Mechanics (QM/MM). The Hamiltonian for the hybrid QM/MM model[16] as implemented in CHARMM[17] was used to simulate the glucose and

$$H = H_{QM} + H_{MM} + H^{Elec}_{QM/MM} + H^{vdW}_{QM/MM} \quad (1)$$

galactose solutions. H_{QM} is the Hamiltonian describing the quantum potential energy for the quantum part of the system while H_{MM} describes the MM potential for the MM part of the system. The interaction between the QM and MM components of the system are described by electrostatic and van der Waals interactions using the $H^{Elec}_{QM/MM}$ and $H^{vdW}_{QM/MM}$ terms.

We use the TIP3P[18] water model as implemented in CHARMM to model the water solvent and a modified PM3 parameter set (PM3CARB-1)[19] to quantum mechanically model the carbohydrate thereby including electronic effects in our PM3CARB-1/TIP3P simulation. We chose the PM3CARB-1 parameter set for several reasons: (i) it shows an improved prediction for intramolecular hydrogen bond strength, important for correctly describing carbohydrates in vacuo and in aqueous solution, (ii) in contrast to PM3, ^{1}C4 ring conformations are correctly ranked by PM3CARB-1 as less favorable than ^{4}C1 conformations, (iii) an underestimation of H−H repulsion, a known limitation in the Gaussian core functions of PM3, appears to be corrected by the PM3CARB-1 model, and (iv) in general it appears to improve ring conformation modeling and energetics when compared to PM3. This modification to PM3 was arrived at by fitting PM3 parameters to match the results of MP2 results for a small set of carbohydrate analogues.[19] The resulting PM3CARB-1 is reported to predict the structure and energies of small carbohydrate analogues more accurately than PM3.[19]

Potential of Mean Force. We calculate the potential of mean force (PMF) as a function of the torsion angle ω, that is the free energy of rotation $W(\omega)$ which is related to the probability density $P(\omega)$ for the hydroxymethyl rotation ω, by

$$W(\omega) = -kT \ln P(\omega) \quad (2)$$

where k is the Boltzmann constant, and T is the temperature in Kelvin. The PMF is derived in a canonical ensemble (constant NVT) to get the Helmholtz free energy for the hydroxymethyl rotation curve. To calculate the PMF, uniform sampling of ω is necessary. For barrier heights that are larger than $3kT$, this is achieved by modifying the potential function $V(\omega)$ with an appropriate biasing potential, $U(\omega)$. The best choice for $U(\omega)$ would be

$$U(\omega) = kT \ln P(\omega) \tag{3}$$

Unfortunately, this is not possible since the probability density distribution can only be computed once the PMF is known. To approach uniform sampling we used a variant of Mezei's adaptive umbrella sampling[20] which we reported earlier.[21] At the start of these calculations the $W(\omega)$ function is unknown. Initially, an unbiased simulation (i.e., $U(\omega) = 0$) is performed. We then use the resulting probability distribution as a first guess of the PMF ($W(\omega)$) from which an improved biasing potential ($U(\omega)$) for the next simulation can be calculated. This process continues iteratively until the ω conformational space is adequately sampled. Adequate sampling is generally accepted to be achieved when a ratio of most sampled to least sampled states is at least 1:50.[22] However, using our adaptive umbrella sampling method, sampling ratios of 1:5 have been calculated resulting in greater accuracy.[23]

At each step in the iterative process, we run several biased simulations and on completing each set of biased simulations we combine all the biased population distributions with the current and previous iterations using computed weighting factors to yield the best unbiased probability distribution, p_k. This procedure is commonly known as the weighted histogram analysis method (WHAM)[24] where

$$p_k = \frac{\sum_i n_{i,k}}{\sum_i N_i f_i c_{i,k}} \tag{4}$$

Here the i^{th} simulation has n_i stored configurations that have been divided into k bins giving a total number of configurations $N_i = \sum_k n_{i,k}$ where $n_{i,k}$ is the histogram for ω from the k^{th} bin. The free energy weighting factors are defined as

$$f_i = \frac{1}{\sum_k e^{-\beta U_i(\omega_k)} p_k} \tag{5}$$

where the umbrella energy weighting factors (U_i) depend on the value of ω that falls in the k^{th} bin (ω_k). The WHAM equations are applied iteratively until the maximum difference (tolerance) between the previous and current iteration weighting coefficients ($\max|f_j^i - f_j^{i-1}|$) is less than 0.001. The accuracy of the free energy surface is a factor of a 100 less accurate than the tolerance chosen.[25]

Molecular Dynamics. In aqueous solution both α- and β-configurations of glucose and galactose exist in the ratio α/β = 1:1.74 (or 36:64) for glucose[26,27] and α/β = 1:2.57 for galactose.[27] We simulated both conformers using CHARMM 33b2[17] although only the β-anomers are shown here due to their preference in aqueous solution. The saccharides were treated with PM3CARB-1 where the initial structures were minimized for 100 steps followed by a 2 ns equilibration at a temperature of 298.15 K. The vacuum calculated PMFs were constructed from twenty simulations of 0.4 ns totaling 8 ns for each saccharide. We applied weak constraints to the pyranoside ring dihedrals to preserve the $^4C_1$ ring conformation. Langevin dynamics combined with a leapfrog-verlet integrator using an integration time step of 1 fs produced the canonical (NVT) ensembles at 298.15 K. The equation of motion

$$\frac{d^2\vec{r}_i(t)}{dt^2} = m_i^{-1}\vec{F}_i + m_i^{-1}\vec{R}_i - \gamma_i \frac{d\vec{r}_i(t)}{dt} \tag{6}$$

where the stochastic term ($\vec{R}_i$) and the frictional force proportional to a frictional coefficient (γ_i) together control the temperature. The frictional coefficient of 62.5 ps^{-1} was applied to all atoms in the gas phase. We found that the random stochastic force used in the Langevin method improved the sampling of conformational space. The CHARMM switching functions were applied on a group-by-group basis between 12 and 14 Å. Nonbonded interactions were updated heuristically.

Solution phase MD simulations were run using the PM3CARB-1[19] semiempirical model for glucose and galactose immersed in a periodic 33.98 Å cubic box containing 1331 equilibrated TIP3P water molecules. Waters overlapping with the monosaccharide were removed resulting in 1318 waters in both the glucose and galactose solutions. The system was then minimized for 1000 steps. The box length was adjusted to 34.11 Å for both saccharides to match an experimental density[27] of 1.006 $g \cdot cm^{-3}$ for these solutions. The SHAKE algorithm[28] was applied to all MM hydrogens. CHARMM implemented switching functions were applied between 12 and 14 Å on a group-by-group basis. Nonbonded and imaging interactions were updated heuristically. The systems were then heated to 298.15 K over 400 ps and equilibrated for 2 ns. Twenty constrained dynamics simulations of 0.8 ns in length were performed to give a total of 16 ns for each monosaccharide solution. Weak constraints were applied to the pyranoside ring dihedrals to prevent the transition from a chair to a boat structure, although this was not expected to occur in solution.

Electron Density and Orbital Analysis Methods. All density functional calculations were performed using GAMESS-UK 7.0.[29] Becke's three parameter exchange functional and Lee−Yang−Parr correlation functional (B3LYP)[30] were employed with restricted closed shell Hartree−Fock for these calculations.

Vacuum rotational energy curves were constructed for glucose and galactose using a multiple-level approach[31] where an ensemble of 200 structures per conformation were extracted from the PM3CARB-1[19] PMF ensemble and averaged single-point energies were computed at the RB3LYP/6-31G* and RB3LYP/6-31+G** levels of theory.

In vacuum, the best orientations of the secondary hydroxyls of the saccharide ring are either all arranged as clockwise or reverse clockwise to achieve the maximum number of intramolecular hydrogen bonds. We used the reverse clockwise ordering as it results in the lowest monosaccharide energy.[32] Each geometry at the gg, gt, and tg stationary points for both carbohydrates were optimized at the RB3LYP/6-31G* and RB3LYP/6-31+G** levels of theory. These basis sets have been shown to produce accurate structures and energies for monosaccharides.[33] The topology of the electron densities for the optimized structures were analyzed using the atoms in molecules (AIM)[34] approach. We searched for minima of the electron density surface in one dimension: the so-called (3,−1) minima or bond critical points. Where the (3,−1) notation signifies that in the three dimensional electron density surface there is a saddle point resulting from electron density maxima in two directions and a minimum in the third direction. These bond critical points are a measure of shared electron density between atoms. Natural bond orbital (NBO)[35] analysis was also carried out so that the wave function could be partitioned into its "most natural" orbitals.

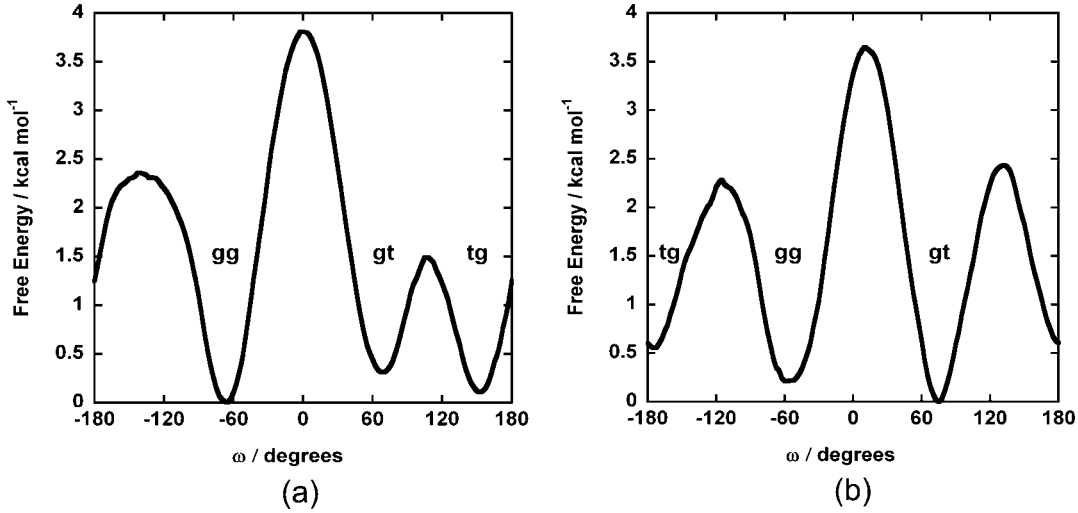

Figure 2. The potential of mean force curves in vacuo for (a) β-D-glucose, (b) β-D-galactose. These were calculated using PM3CARB-1 with weak constraints applied to the pyranoside ring.

TABLE 1: Minima Conformation Vacuum Populations and the NBO Overlap Contributions and Deviations from the Minima for β-D-Glucose and β-D-Galactose

β-D-glucose				
rotamer	normalized populations	total NBO overlap for $\sigma_{C6\text{-}H}\rightarrow\sigma^*_{C5\text{-}O5}$ and $\sigma_{C5\text{-}H}\rightarrow\sigma_{C6\text{-}O6}$ at ω-$\Delta\omega$ (kcal·mol^{-1})	total NBO overlap for $\sigma_{C6\text{-}H}\rightarrow\sigma^*_{C5\text{-}O5}$ and $\sigma_{C5\text{-}H}\rightarrow\sigma_{C6\text{-}O6}$ at ω (kcal·mol^{-1})	total NBO overlap for $\sigma_{C6\text{-}H}\rightarrow\sigma^*_{C5\text{-}O5}$ and $\sigma_{C5\text{-}H}\rightarrow\sigma_{C6\text{-}O6}$ at ω+$\Delta\omega$ (kcal·mol^{-1})
gg	40	8.73	10.31	7.65
gt	22	6.27	7.04	7.45
tg	32	4.59	2.94	0.56
β-D-galactose				
rotamer	normalized populations	total NBO overlap for $\sigma_{C6\text{-}H}\rightarrow\sigma^*_{C5\text{-}O5}$ and $\sigma_{C5\text{-}H}\rightarrow\sigma_{C6\text{-}O6}$ at ω-$\Delta\omega$ (kcal·mol^{-1})	total NBO overlap for $\sigma_{C6\text{-}H}\rightarrow\sigma^*_{C5\text{-}O5}$ and $\sigma_{C5\text{-}H}\rightarrow\sigma_{C6\text{-}O6}$ at ω (kcal·mol^{-1})	total NBO overlap for $\sigma_{C6\text{-}H}\rightarrow\sigma^*_{C5\text{-}O5}$ and $\sigma_{C5\text{-}H}\rightarrow\sigma_{C6\text{-}O6}$ at ω+$\Delta\omega$ (kcal·mol^{-1})
gg	37	10.56	12.1	6.67
gt	44	4.97	7.17	5.93
tg	17	2.84	0.84	2.28

Results and Discussion

Previous studies have postulated that the major reason for the conformational preferences of the hydroxymethyl group in glucose and galactose is due to the gauche effect. A useful definition of the gauche effect is "there is a stereoelectronic preference for conformations in which the best donor lone pair or bond is antiperiplanar to the best acceptor bond".[14] While this preference is attributed to favorable interactions between a bonding orbital (σ) and an antibonding orbital (σ^*) it does not explain the ordering of the glucose conformations or the different ordering in galactose that arises from a hydroxyl configurational change at the C4 position. For these reasons, we calculated the vacuum and solution free energy profiles for both glucose and galactose and investigated the relative free energies and electronic structures of the hydroxymethyl in the gg, gt, and tg conformations.

Vacuum Conformational Preferences. The relative free energy profiles of rotation about the ω-torsion angle for glucose and galactose in vacuum are shown in Figure 2. The PMFs are well converged with sampling ratios of least to most sampled conformers in the glucose simulation being 1.6:1 and for the galactose simulation being 4.5:1. A comparison of the gg (0.00 kcal mol^{-1} at $-65.0°$), tg (0.10 kcal mol^{-1} at 152.5°), and gt (0.31 kcal mol^{-1} at 70°) conformers for glucose show minimal differences in their free energies. Similarly the differences in free energies between the galactose conformers gg (0.21 kcal mol^{-1} at $-57.5°$), gt (0.00 kcal mol^{-1} at 75.0°), and tg (0.55 kcal mol^{-1} at $-172.5°$) are less than 1 kcal mol^{-1}.

The population of each well minimum (i.e., gg, gt, tg) of the free energy curve can be calculated by summing the populations in between the well boundaries. The boundary between a well population and a transition population is defined as the point where the first derivative of the free energy is at its turning point, i.e., where $d^2A/d\omega^2 = 0$. The gas phase population distribution for glucose and galactose were calculated in this way (Table 1) and gave population distributions of gg/gt/tg = 40:22:32 for glucose and gg/gt/tg = 37:44:17 for galactose.

The RB3LYP/6-31G*//PM3CARB-1 and RB3LYP/6-31+G**//PM3CARB-1 gas phase ω-torsion curves are shown in Figure 3 for both glucose and galactose. We find for glucose that the smaller basis set gives a lower energy for the tg conformer compared with the larger basis set and has an overall gg/gt/tg energy that is similar to the predictions of the PM3CARB-1 PMF. However, this is not a fair comparison as the PMF includes entropic factors such as the configuration of secondary alcohol rotations as well as bond and angle configurations for the entire monasaccharide. None the less from this we see that for glucose the addition of diffuse functions lowers the preference for tg relative to gg by 2.83 kcal·mol^{-1} and the barrier heights between gg to gt and tg to gg increase by 2.11 kcal·mol^{-1} and 0.55 kcal·mol^{-1}, respectively.

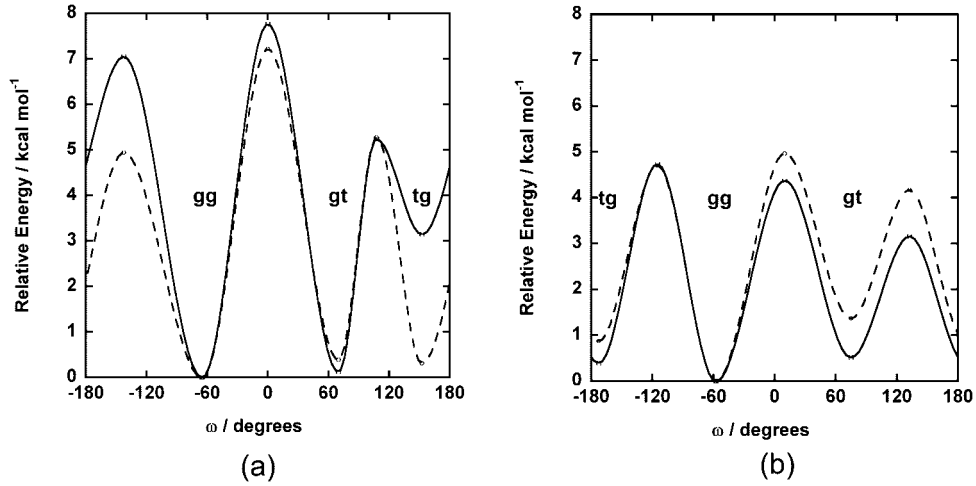

Figure 3. Primary alcohol torsional profile for a) β-D-glucose and b) β-D-galactose at the basis sets RB3LYP/6-31G*//PM3CARB-1 (solid line) and RB3LYP/6-31+G**//PM3CARB-1 (broken line).

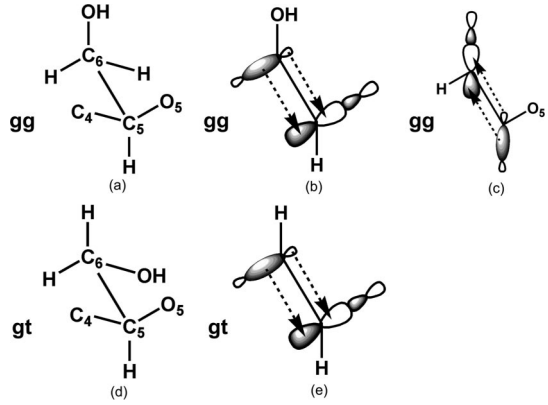

Figure 4. (a) A sawhorse-type projection of the atoms connected to the C5−C6 bond. (b) Illustration of donation of electron density from $\sigma_{C6-H} \rightarrow \sigma^*_{C5-O5}$ in the gg rotamer. (c) Illustration of donation of electron density from $\sigma_{C5-H} \rightarrow \sigma^*_{C6-O6}$ in the gg rotamer. (d) A sawhorse-type projection of the atoms connected to the C5−C6 bond. (e) Illustration of donation of electron density from $\sigma_{C6-H} \rightarrow \sigma^*_{C5-O5}$ in the gt rotamer. (f) Illustration of donation of electron density from $\sigma_{C5-H} \rightarrow \sigma^*_{C6-O6}$ in the gt rotamer.

We optimized gg, gt, and tg conformations for glucose and galactose at the RB3LYP/6-31G* and RB3LYP/6-31+G** levels of theory and then used NBO and AIMs analysis to investigate the electronic reasons underlying the conformational preferences. The most important orbital interactions are the bonding orbital to antibonding orbital interactions between the C−H and C−O orbitals, specifically $\sigma_{C6-H} \rightarrow \sigma^*_{C5-O5}$ and $\sigma_{C5-H} \rightarrow \sigma^*_{C6-O6}$. These orbital interactions for the gg and gt conformers in glucose and galactose are shown in Figure 4. They stabilize the conformers in the order gg > gt > tg (Table 1) for both molecules. In the gg conformer, the best donor and acceptor bonds are anti to one another, that is C6−H (a good bonding donor) is opposite to C5−O5 (a good antibonding acceptor), and at the same time C5−H (a good bonding donor) is opposite to C6−O6 (a good antibonding acceptor) (Figure 4b,c). This NBO stabilization interaction analysis is consistent with the gauche effect. It is likely that the stabilization effect from the $\sigma_{C6-H} \rightarrow \sigma^*_{C5-O5}$ and $\sigma_{C5-H} \rightarrow \sigma^*_{C6-O6}$ interaction may change as we deviate from the low energy stationary points of the PMF. The NBO energies were calculated at each minima and where $d^2A/d\omega^2 = 0$, i.e., at maximum deviation from the specific minima. These values are shown in Table 1. The greatest overlap occurs for the glucose gauche conformer gg and both galactose gauche conformers gg and gt at the angles yielding the most favorable free energy.

The energy profiles of the hydroxymethyl moiety of multiple glycero-hexopyranoside rings (i.e., dehydroxylated glucose rings)[12] have been investigated where the hydrogen of the 6-hydroxy group was explicitly turned away so that no intramolecular hydrogen bonds could be formed. These conformers were then compared with those that could form intramolecular hydrogen bonds from O6−H to O5 leading to the conclusion that hydrogen bonding was the reason for a gg and gt preference. This and further studies[15,36,37] postulated that these intramolecular hydrogen bonds were the primary reason for the gauche preferences observed in monosaccharides.

We used the AIMs approach to analyze the electron densities of RB3LYP/6-31G* and RB3LYP/6-31+G** optimized structures to determine the extent and nature of intramolecular hydrogen bonding that involve the hydroxymethyl group in glucose and galactose. There are eight criteria, detailed by Popelier,[38,39] that should be met to characterize a hydrogen bond; however, satisfying only one of these conditions would be sufficient to define a hydrogen bond.[38] We considered the existence of a bond critical point with electron density (ρ) between 0.002 and 0.035 au as indicative of a hydrogen bond.

We found a (3,−1) bond critical point between O4 and O6−H for the glucose tg and the galactose gg conformers indicating a hydrogen bond where O6 is the donor and O4 the acceptor. The bond critical points for tg glucose has $\rho = 0.0244$ au and for gg galactose $\rho = 0.0251$ au. There are no other hydrogen bonds involving the hydroxymethyl group. In galactose there is a hydrogen bond formed between the axial 4-hydroxyl and equatorial 3-hydroxyl for the gg, gt, and tg conformations. The 4-hydroxyl to 3-hydroxyl hydrogen bond has similar electron densities for all minima; $\rho_{gg} = 0.0190$ au, $\rho_{gt} = 0.0196$ au, $\rho_{tg} = 0.0204$ au. These ρ are within the range expected for hydrogen bonding.[38,39]

Either the 4-hydroxyl or the 6-hydroxyl hydrogens can be donors. To measure the orientational preference of the 4-hydroxyl and the 6-hydroxyl hydrogens relative to each other for the vacuum trajectory we use the torsion angle θ = H6−O6−C6−C5 and a pseudotorsion angle η = H4−O4−C4----C6. We illustrate the torsional angle θ and the pseudo torsion angle η for the glucose tg conformer in Figure 5a and the galactose gg conformer in Figure 5b. The angles θ and η were chosen as they easily show the direction in which the hydrogen of the

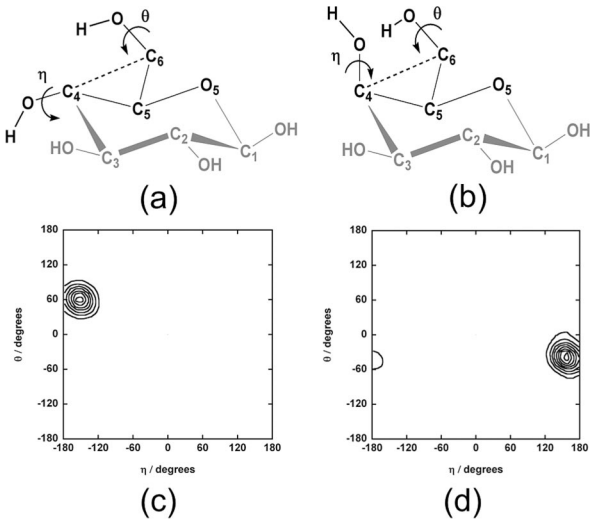

Figure 5. (a) Illustrations of the potential interactions between the 4-hydroxyl and 6-hydroxyl group of the tg conformer of β-D-glucose when rotating the θ- and η-torsional angles (H6−O6−C6−O5 and H4−O4−C4−C6, respectively). (b) The same as for panel a but for the gg conformer of β-D-galactose. (c) H-bond 2D vacuum contour plot for β-D-glucose. Every contour is a 10% increment of the maximum density. The data has had one smoothing pass applied to it. (d) The same as for panel c but for the gg conformer of β-D-galactose.

hydroxyl groups are pointing. The (θ,η) probability distributions for the tg glucose (Figure 5c) and gg galactose (Figure 5d) vacuum trajectories reveal that for both molecules the 6-hydroxyl group is the hydrogen bond donor. Specifically, the most probable configuration for glucose is the (65, −155) orientation while the most probable galactose configuration is the (−40,155) orientation. Inspection of the NBO analysis shown in Table 1 for gg and gt conformers shows that the gg conformer receives stabilization of more than 3 to 5 kcal mol^{-1} compared with the gt from the gauche effect. Combining the population distribution data from the QM/MM trajectory and the AIMs analysis of the RB3LYP/6-31G* and RB3LYP/6-31+G** optimized structures we conclude that the enhanced stability of the tg glucose and the gg galactose conformers is due to O6−H----O4 intramolecular hydrogen bonds having significant covalent (directional) character.

In vacuum the intrinsic stereoelectronic $\sigma_{C6-H} \rightarrow \sigma^*_{C5-O5}$ and $\sigma_{C5-H} \rightarrow \sigma^*_{C6-O6}$ interactions that favor the gauche conformer in glucose marginally overcomes the intramolecular hydrogen bond that stabilizes the tg conformer resulting in the population trend gg > tg > gt. The stereoelectronic $\sigma_{C6-H} \rightarrow \sigma^*_{C5-O5}$ and $\sigma_{C5-H} \rightarrow \sigma^*_{C6-O6}$ interactions and the hydrogen bond that favor the gauche conformer in galactose is counterbalanced by the steric repulsion it experiences stemming from the 1,3 syn-diaxial interactions and unfavorable dipole−dipole interactions between O4, O5, O6.[15,37] The overall population trend for galactose is therefore gt > gg > tg. However the population distributions derived from vacuum rotational free energies of the hydroxymethyl conformations for both glucose and galactose are not in agreement with experimental solution NMR results. The conformational preferences of the hydroxymethyl group in monosaccharides therefore cannot be exclusively rationalized in terms of intramolecular electronic effects but must in some way rely on the solvent.

Solution Conformational Preferences. The relative free energy curves for the rotation about the ω-torsion angle for glucose and galactose in water are shown in Figure 6a,b, respectively. The PMFs are well converged for both systems where for glucose the ratio of most to least sampled conformers is 6.8:1 and for galactose it is 4.8:1. The glucose minimum energy conformations are gt (0.00 kcal·mol^{-1} at 70°), gg (0.10 kcal·mol^{-1} at −67.5°), and tg (1.09 kcal·mol^{-1} at 150°). The free energy curve for glucose upon solvation displays a significantly different low energy conformational ranking than it did in vacuum. The gt conformer is now the lowest energy conformer and the gg and tg conformers have greater free energies compared with the rotamers in vacuum. The tg conformer has changed by 0.99 kcal·mol^{-1} relative to the lowest energy conformer. Moreover, the barrier heights separating the minima are different from the vacuum case where the gg−gt barrier is lowered by 0.63 kcal·mol^{-1}, the gt−tg barrier is 0.25 kcal·mol^{-1} lower, and the tg−gg barrier has increased by 1.33 kcal·mol^{-1}.

The population distribution for each conformer well in the solution hydroxymethyl PMFs is calculated using the same prescription as described for the vacuum PMFs. In the case of glucose gg/gt/tg ratios are 35:57:3 indicating that the gt conformer is most favored in solution. This agrees very well with experimental NMR values reported by Stenutz[2] (41:52:7) where they used their newly developed Karplus equations for $^2J_{HH}$ and $^3J_{HH}$ to establish the rotamer distribution. However, both our values and those of Stenutz et al.[2] differ with the Bock et al.[40] (52:41:7) and Nishida et al.[1,41] (53:45:2) reported distributions for gg/gt/tg where they used older forms of the Karplus equations.

Solvation of galactose also has a significant effect on the free energy of rotation for the hydroxymethyl group. The minimum energy conformers are gt (0.00 kcal·mol^{-1} at 70°), tg (1.00 kcal·mol^{-1} at 172.5°), and gg (1.32 kcal·mol^{-1} at −57.5°). While gt remains the lowest energy conformer, gg (increased by 1.11 kcal·mol^{-1}) and tg (increased by 0.45 kcal·mol^{-1}) have exchanged energetic order in the free energy profile. The gg−gt barrier remains more or less the same while the gt−tg barrier decreased by 0.44 kcal·mol^{-1} and the tg−gg barrier increased sharply by 1.56 kcal·mol^{-1}. Extracting the gg/gt/tg population distributions for galactose from the PMF gives 4:86:7. This distribution agrees reasonably well with the aqueous solution preference determined from the NMR experiments of Stenutz[2] (3:67:30) and Nishida[1] (18:61:21).

Stereoelectronic versus Solvent Effects. To understand the conformational preferences of glucose and galactose in solution we weigh up the intramolecular stabilization and destabilization originating from stereoelectronic effects and hydrogen bonding against the stabilization and destabilization effects that the water molecules have on the gg, gt, and tg conformers. To simplify the discussion, we summarized this in Table 2. We found via NBO analysis that the $\sigma_{C6-H} \rightarrow \sigma^*_{C5-O5}$ and $\sigma_{C5-H} \rightarrow \sigma^*_{C6-O6}$ interactions (shown in Figure 4a−e) stabilized the gg conformer for both monosaccharides by more than 10 kcal mol^{-1}. Although there is gauche stabilization present from $\sigma_{C6-H} \rightarrow \sigma^*_{C5-O5}$ (5.5 kcal mol^{-1}) in the gt conformation there is less than 1 kcal mol^{-1} originating from $\sigma_{C5-H} \rightarrow \sigma^*_{C6-O6}$ interaction. The tg conformation has a minor (∼2.5 kcal mol^{-1}) stabilization from the $\sigma_{C6-H} \rightarrow \sigma^*_{C5-O5}$ interaction resulting in an overall gg > gt > tg preference for both monosaccharides attributable to the gauche stereoelectronic interactions.

The (θ,η) probability distributions for the tg glucose (Figure 7a) and gg galactose (Figure 7b) solution trajectories reveal that for both molecules several orientations are sampled. The glucose OH6 and OH4 hydroxyls rotate more freely with a preference for configurations centered about (80,−140), (70,100) and (−70,80) while in the case of galactose there are preferred

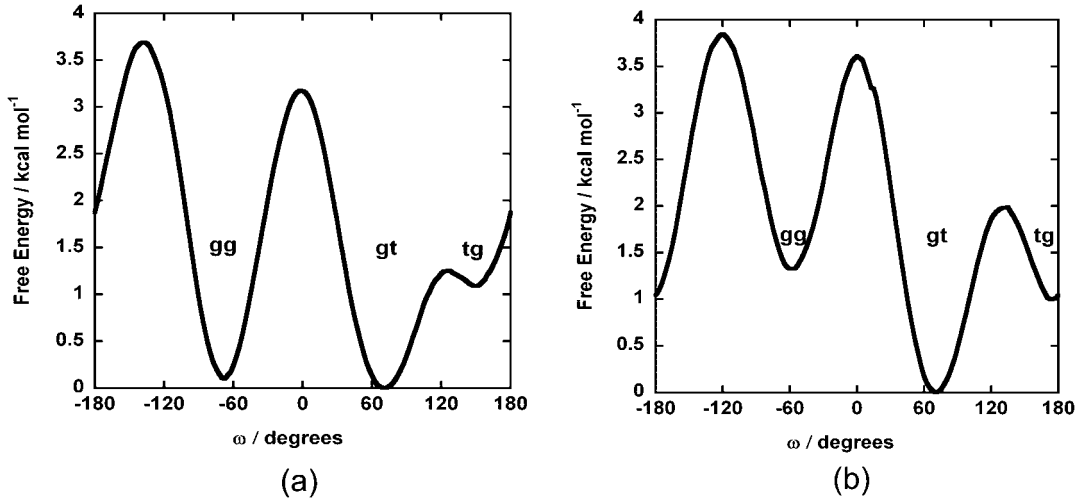

Figure 6. The potential of mean force in the aqueous phase for (a) β-D-glucose and (b) β-D-galactose calculated using PM3CARB-1/TIP3P with weak constraints applied to the pyranoside ring.

TABLE 2: Conformational Stabilizing and Destabilizing Effects Originating from within β-D-Glucose and β-D-Galactose and Their Interactions with Water[a]

	glucose				galactose			
	internal		solvent		internal		solvent	
rotor	stable	unstable	stable	unstable	stable	unstable	stable	unstable
gg	G(s)			HB(s)	G(s)	SR(s)		HB(s)
gt	HB(s) G(m)	SR(w)	BHB(s)	HB(w)	HB(s) G(m)	SR(w)	BHB(s)	HB(w)
tg	HB(w)	SR(w)	BHB(m)	HB(w)			BHB(s)	HB(w)

[a] HB = hydrogen bonding, BHB = bridging hydrogen bonds, G = gauche stabilization from $\sigma_{C6-H} \rightarrow \sigma^*_{C5-O5}$ and $\sigma_{C5-H} \rightarrow \sigma^*_{C6-O6}$ interactions, SR = steric repulsion due to lone pair interactions between oxygens. The weak (w), medium (m), and strong (s) symbols in brackets indicate the strength of the effect.

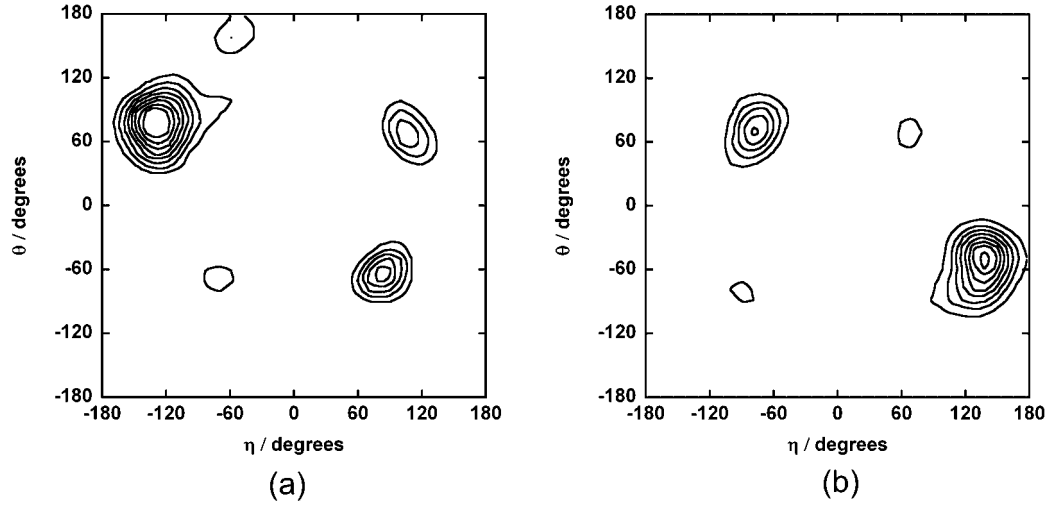

Figure 7. H-bond 2D water contour plot for (a) tg conformer of β-D-glucose and (b) gg conformer of β-D-galactose. Every contour is a 10% increment of the maximum density with the central contour representing the most probable configuration. The data has had 1 smoothing pass applied to it.

configurations distributed about two centers (70,−80) and (−50,140). The nonbonded orbitals on the O4 and O6 oxygen atoms for the gg galactose conformation centered at (70,−80) are positioned for repulsive interactions and destabilize the gg conformation.

In discussing hydrogen bonds involving the hydroxymethyl group, we distinguish the functional group "donating" the hydrogen bond (D) from the one accepting it (A). We used a geometric distance (D...A < 3.5A) and angle (180° < DHA < 120°) criteria to detect if there are internal hydrogen bonds of moderate strength between C4 hydroxyls or the ring ether O5 and the hydroxymethyl group in glucose and galactose over MD trajectories (2ns in length) for each system. We define a function $C(t,t_i;t^*)$, which takes the value 1 if the distance between oxygens of functional groups is at least 3.5 Å and the O−H---O angle fulfils the above criterion. These conditions must be met for both time frames t_i and $t_i + t$ and in the interim the hydrogen bond must not be broken for any continuous period, longer than t^*. Otherwise it takes on a value of 0. In the case of waters that are participating in bridging hydrogen bonds between the two functional groups, a water molecule is considered to form a bridging hydrogen bond (BHB) if its oxygen satisfies the above

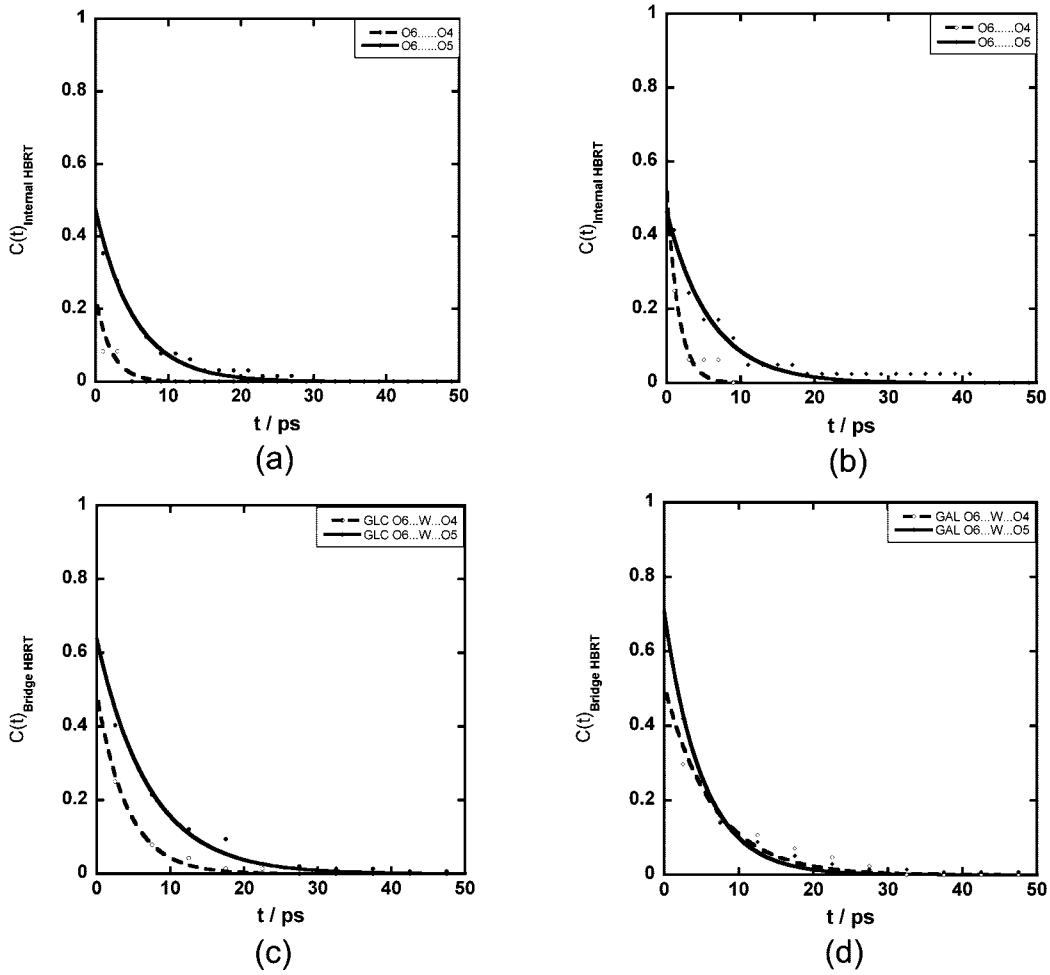

Figure 8. Hydrogen bond number correlation functions ($C(t)$) along with exponential fits to $C(t)$ (a) between the O6 and O5 (—) and O6 and O4 (----) for β-D-glucose, (b) between the O6 and O5 (—) and O6 and O4 (----) for β-D-galactose, (c) for waters forming hydrogen bond bridges between the O6 and O5 (—) and O6 and O4 (----) for β-D-glucose, and (d) for waters forming hydrogen bond bridges between the O6 and O5 (—) and O6 and O4 (----) for β-D-galactose.

distance criteria to each of the oxygen atoms on the monosaccharide's functional groups. The parameter t^* is introduced to ignore cases when the hydrogen bond temporarily breaks and reforms or in the case of water if the solvent molecule does not properly enter the bulk solution. We use a value of $t^* = 2$ ps, which has been used in studies of hydration shell lifetimes and sizes around ions.[42] Consequently a normalized function that gives a probability of an intramolecular hydrogen bond or intermolecular hydrogen bond (in the case of a water molecule participating in a BHB) lasting for time t is defined here in equation 7.

$$C(t) = \frac{\langle P_j(t, t_i; t^*)\rangle}{\langle P_j(0, t_i; t^*)\rangle} \tag{7}$$

Plots of $C(t)$ vs time for both glucose and galactose are shown in Figure 8. The intramolecular hydrogen bonds between the hydroxymethyl group and the O5 persists (solid lines in Figure 8a,b) for much longer than those made with the hydroxyl on C4 (broken lines in Figure 8a,b). These $C(t)$ curves for the intramolecular hydrogen bonds moderately correlate ($85\% < R < 98\%$) to exponential fits of the form $\exp(-t/\tau)$ where τ is the residence time. The $C(t)$ data is shown along with the curve for the exponential fitting function in Figure 8. The residence times for the hydrogen bonds (between C4 and C6 hydroxyls) in glucose tg and galactose gg are 2 ps while the residence times for the hydrogen bond (between the primary alcohol and O5 ring oxygen) stabilizing the gt conformation in glucose and galactose are 5 and 6 ps respectively. From this we infer that the glucose tg and galactose gg conformations are weakly stabilized by intramolecular hydrogen bonding involving the hydroxymethyl group. This is compared to the moderate stabilization of the gt conformations in both monosaccharides due to hydroxymethyl group intramolecular hydrogen bonding.

A molecular mechanics force field study on methoxylated gluco- and galacto-pyranosides in different solvents showed that intramolecular hydrogen bonding is weakened in water.[43] They further postulated that only solvation correctly reproduces the hydroxymethyl preferences observed in NMR experiments.[44] Previously we established that intramolecular hydrogen bonds are energetically similar to carbohydrate−water hydrogen bonds having less than 1 kcal mol^{-1} difference between them.[45] In addition it has been more generally argued that solvent polarity appears to affect the rotameric distribution of the hydroxymethyl group.[37,46] The ability of a polar solvent such as water to reduce intramolecular hydrogen bonding was observed in NMR experiments conducted by De Vries and Buck.[37] They measured the NMR signal in a saccharide-$CDCl_3$ solution and found that the relatively nonpolar $CDCl_3$ solvent showed line broadening which is indicative of intramolecular hydrogen bonding. Upon addition of the polar water solvent the broadening disappeared. In our

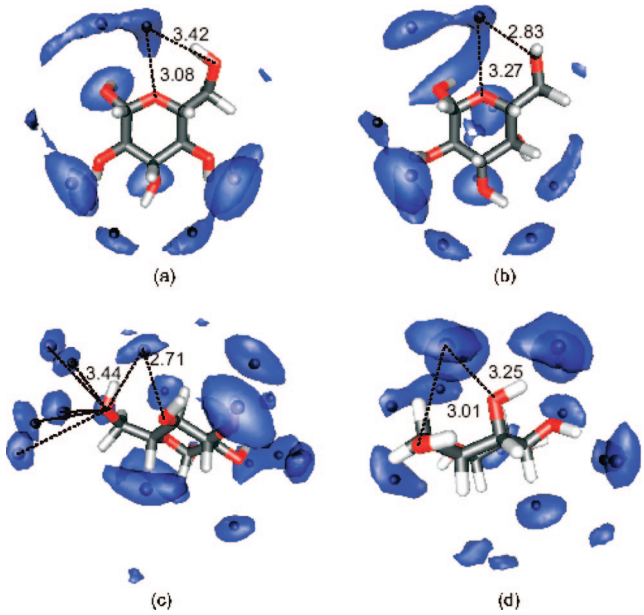

Figure 9. Spatial distribution functions for water probability densities about the hydroxymethyl group in (a) the gt conformation for glucose, (b) the gt conformation for galactose, (c) the tg conformation for glucose, and (d) the tg conformation for galactose.

estimation disruption of the intramolecular hydrogen bonding interaction lowers the preference for the tg conformer of glucose by 0.99 kcal mol^{-1} and the gg conformer of galactose by 1.11 kcal mol^{-1}. This observation provides evidence for the conjecture made previously by Grindley and Rockwell[46] that the solvent caused a loss of intramolecular hydrogen bonding from the OH6 to O4 which was the underlying reason for the decrease in population of the tg rotamer in glucose.

A major reason for the stability of the gauche hydroxymethyl conformers is the gauche effect (Table 1 and Figure 4). The gt conformers gain additional stability in solution compared with the gg conformations because of longer lived intramolecular hydrogen bonds. Particularly in the case of the galactose water solution there is significant loss of intramolecular hydrogen bonding in the gg conformer (Figure 8b) making it is less stable in water (Figure 6) than in vacuum (Figure 2). This explains the decrease in preference for gg compared with gt.

We analyzed the extent to which water forms hydrogen bond bridges between the HO6 hydroxyl and the ring oxygen (O5) and the HO6 hydroxyl and the HO4 hydroxyl in both glucose and galactose. The duration of a BHB formed by a single water between the hydroxymethyl group and the O5 ring oxygen in the gt conformation can be measured by calculating the residence time of the BHB. For this we use the function $C(t,t_i;t^*)$ as described in eq 7 above. These waters participate in moderate to strong BHBs between the two functional groups. Plots of $C(t)$ versus time for glucose and galactose are shown in Figure 8c,d, respectively. The residence times for the BHBs between O6 and O5 in the glucose gt conformer (Figure 8c solid line) is 7.1 ps and for the galactose gt conformer (Figure 8d solid line) is 6.5 ps.

The BHBs formed between O6 and O4 are surprisingly long-lived and strong. To better understand this, we calculated spatial distribution functions (SDFs) as defined and described elsewhere[47] for gg, gt, and tg in each of the monosaccharides. Both gg conformers displayed no water probability densities that are consistent with BHBs. Therefore in Figure 9 we only show the water probability densities for glucose and galactose gt and tg conformations derived from the SDFs at 40% above bulk water probability. The maximum water probability densities are represented as dark spheres within the contours. It can be concluded from the SDFs of the tg conformers for glucose (Figure 9c) and galactose (Figure 9d) and $C(t)$ plots of BHBs formed between O6 and O4 in glucose (Figure 8c broken line) and galactose (Figure 8d broken line) that the tg conformations are further stabilized by water mediated BHBs. The galactose gg conformer however is not stabilized by BHBs in water or intramolecular hydrogen bonding as observed in vacuum but from the gauche effect. However, due to frequent hydrogen bonds made by the hydroxymethyl group and the O4 hydroxyl to surrounding water molecules the lone pairs on the O6 and O4 atoms are unfavorably positioned as can be seen by the (θ,η) distribution (Figure 7b) this leads to steric repulsion between oxygens. This repulsive interaction is the reason for the significant lowering of gg populations in solution compared with those in vacuum and so explains why it is the least favored galactose conformer in water (Figure 6b).

Conclusions

The contributions to conformer stability from stereoelectronic, intramolecular hydrogen bonding, and bridging hydrogen bond factors along with the contributions to their instability from steric repulsion and intermolecular hydrogen bonding with the solvent have been summarized in Table 2. The gauche effect explains why the glucose gg conformer is most populous in vacuum. The strong long-lived intramolecular hydrogen bonds between the HO6 hydroxyl and the HO4 hydroxyl of the tg conformer makes it a more favorable conformer than gt despites the latter's gauche stabilization. Therefore the change in preferential population from gg > tg > gt in glucose vacuum to gt > gg > tg in a glucose-water solution is primarily due to the intramolecular hydrogen bond and the strong and long-lived water BHBs formed between the HO6 hydroxyl and the O5 ring oxygen in the gt conformation.

The preferred galactose hydroxymethyl population changes from gt > gg > tg in vacuum to gt > tg > gg in water. The primary reasons are the following: in water the gt conformer is stabilized by an intramolecular hydrogen bond and bridging waters between the HO6 hydroxyl and the O5 ring oxygen while the gg conformer's unfavorable 1,3 syn-diaxial and dipole−dipole interactions are no longer moderated by strong intramolecular hydrogen bonds as in the vacuum case. As with the glucose tg conformer, solvation of the galactose gg conformer results in a disruption of intramolecular hydrogen bonds between the HO6 hydroxyl and the HO4 hydroxyl. Although the gg conformer has the favorable hyperconjugative $\sigma_{C6-H} \rightarrow \sigma^*_{C5-O5}$ and $\sigma_{C5-H} \rightarrow \sigma^*_{C6-O6}$ resonance the unfavorable steric and dipole−dipole interactions dominate in this conformer reducing its preference. The galactose tg conformer is stabilized by bridging waters between the HO6 and HO4 hydroxyls significantly increasing the sampling of this conformer.

Acknowledgment. This work is based upon research supported by the South African Research Chairs Initiative (SARChI) of the Department of Science and Technology and the National Research Foundation (NRF) awarded to K.J.N. K.J.N. thanks Jiali Gao for helpful discussions. C.B. would like to thank Richard Matthews for assistance with the figures and tables during his absence from UCT; furthermore he thanks the National Research Foundation (Pretoria) for M.Sc. fellowship support and UCT for additional funding.

References and Notes

(1) Nishida, Y.; Ohrui, H.; Meguro, H. *Tetrahedron Lett.* **1984**, *25*, 1575.

(2) Stenutz, R.; Carmichael, I.; Widmalm, G.; Serianni, A. S. *J. Org. Chem.* **2002**, *67*, 949.

(3) Nishida, Y.; Hori, H.; Ohrui, H.; Meguro, H. *Carbohydr. Res.* **1987**, *170*, 106.

(4) Rao, V.; Perlin, A. S. *Can. J. Chem.* **1983**, *61*, 2688.

(5) Larsson, E. A.; Ulicny, J.; Laaksonen, A.; Widmalm, G. *Org. Lett.* **2002**, *4*, 1831.

(6) Lemieux, R. U.; Brewer, T. J. Conformational preferences of solvated hydroxymethyl groups in hexopyranose structures. In *Carbohydrates in solution*; Gould, R., Ed.; American Chemical Society: Washington, DC, 1973; Vol. 117, p 121.

(7) Ohrui, H.; Nishida, Y.; Higuchi, H.; Hori, H.; Meguro, H. *Can. J. Chem.* **1987**, *65*, 1145.

(8) Duus, J. Ø.; Gotfredsen, C. H.; Bock, K. *Chem. Rev.* **2000**, *100*, 4589.

(9) Barrows, S. E.; Storer, J. W.; Cramer, C. J.; French, A. D.; Truhlar, D. G. *J. Comput. Chem.* **1998**, *19*, 1111.

(10) Brady, J. W. *J. Am. Chem. Soc.* **1989**, *111*, 5155.

(11) Cramer, C. J.; Truhlar, D. G. *J. Am. Chem. Soc.* **1993**, *115*, 5745.

(12) Tvaroska, I.; Carver, J. P. *J. Phys. Chem. B* **1997**, *101*, 2992.

(13) Woodcock, H. L.; Brooks, B. R.; Pastor, R. W. *J. Am. Chem. Soc.* **2008**, *130*, 6345.

(14) (a) Thatcher, G. R. J. *The Anomeric effect and associated stereoelectronic effects.- Scope and Controversy.* ACS Symposium Series 539; American Chemical Society: Washington, DC, 1993; Vol. 539, p 6; (b) Kirby, A. J. *The anomeric effect and related stereoelectronic effects at oxygen*; Springer-Verlag: Heidelberg, 1983.

(15) Tvaroska, I.; Taravel, F. R.; Utille, J. P.; Carver, J. P. *Carbohydr. Res.* **2002**, *337*, 353.

(16) Field, M. J.; Bash, P. A.; Karplus, M. *J. Comput. Chem.* **1990**, *11*, 700.

(17) Brooks, B. R.; Bruccoleri, R. E.; Olafson, B. D.; States, D. J.; Swaminathan, S.; Karplus, M. *J. Comput. Chem.* **1983**, *4* (2), 187.

(18) (a) Steinbach, P. J.; Brooks, B. R. *J. Comput. Chem.* **1993**, *15*, 667. (b) Jorgensen, W. L.; Jenson, C. *J. Comput. Chem.* **1998**, *19*, 1179.

(19) McNamara, J. P.; Muslim, A.; Abdel-Aal, H.; Wang, H.; Mohr, M.; Hillier, I. H.; Bryce, R. A. *Chem. Phys. Lett.* **2004**, *394*, 429.

(20) Mezei, M. *J. Comput. Phys.* **1987**, *68*, 237.

(21) Naidoo, K. J.; Brady, J. W. *J. Am. Chem. Soc.* **1999**, *121*, 2244.

(22) Rajamani, R.; Naidoo, K. J.; Gao, J. *J. Comput. Chem.* **2003**, *24*, 1775.

(23) (a) Kuttel, M. M.; Naidoo, K. J. *Carbohydr. Res.* **2005**, *340*, 875. (b) Kuttel, M. M.; Naidoo, K. J. *J. Phys. Chem. B* **2005**, *109*, 7468.

(24) (a) Kumar, S.; Bouzida, D.; Swendsen, R. H.; Kollman, P. A.; Rosenberg, J. M. *J. Comput. Chem.* **1992**, *13*, 1011. (b) Kumar, S.; Rosenberg, J. M.; Bouzida, D.; Swendsen, R. H.; Kollman, P. A. *J. Comput. Chem.* **1995**, *16*, 1339. (c) Kumar, S.; Payne, P. W.; Vásquez, M. *J. Comput. Chem.* **1996**, *17*, 1269.

(25) Ghosh, I.; McCammon, J. A. *Biophys. J.* **1987**, *51*, 637.

(26) Mason, P. E.; Neilson, G. W.; Enderby, J. E.; Saboungi, M. L.; Brady, J. W. *J. Phys. Chem. B* **2005**, *109*, 13104.

(27) *CRC Handbook of Chemistry and Physics*, 61st ed.; Weast, R. C., Ed.; CRC Press: Boca Raton, FL, 1974.

(28) van Gunsteren, W. F.; Berendsen, H. J. C. *Mol. Phys.* **1977**, *34*, 1311.

(29) Guest, M. F.; Bush, I. J.; van Dam, H. J. J.; Sherwood, P.; Thomas, J. M. H.; van Lenthe, J. H.; Havenith, R. W. A.; Kendrick, J. *Mol. Phys.* **2005**, *103*, 719.

(30) (a) Becke, A. D. *J. Chem. Phys.* **1993**, *98*, 5648;(b) Lee, C.; Yang, W.; Parr, R. G. *Phys. Rev. B* **1988**, *37*, 785.

(31) Corchado, J. C.; Truhlar, D. G. *Dual-level methods for electronic structure calculations of potential energy functions that use quantum mechanics as the lower level*; Gao, J., Thompson, M. A., Eds.; American Chemical Society: Washington, DC, 1998; Vol. 712; p 106.

(32) Polavarapu, P. L.; Ewig, C. S. *J. Comput. Chem.* **1992**, *13*, 1255.

(33) Brown, J. W.; Wladkowski, B. D. *J. Am. Chem. Soc.* **1996**, *118*, 1190.

(34) (a) *Bader Atoms in Molecules - A Quantum Theory*; Oxford University Press: Oxford, 1990. (b) Biegler-König, F.; Schönbohm, J.; Bayles, D. *J. Comput. Chem.* **2001**, *22*, 545. (c) Biegler-König, F.; Schönbohm, J. *J. Comput. Chem.* **2002**, *23*, 1489.

(35) (a) *NBO*, version 3.1 (computer program). Institute of Theoretical Chemistry, University of Wisconsin: Madison, WI. (b) Weinhold, F.; Landis, C. *Valency and Bonding. A Natural Bond Orbital Donor-Acceptor Perspective*; Cambridge University Press: Cambridge, 2005.

(36) Wladkowski, B. D.; Chenoweth, S. A.; Jones, K. E.; Brown, J. W. *J. Phys. Chem. A* **1998**, *102*, 5086.

(37) de Vries, N. K.; Buck, H. M. *Carbohydr. Res.* **1987**, *165*, 1.

(38) Koch, U.; Popelier, P. L. A. *J. Phys. Chem.* **1995**, 9747.

(39) Popelier, P. L. A. *J. Phys. Chem. A* **1998**, *102*, 1873.

(40) Bock, K.; Guzman, J. B. F.; Ogawa, S. *Carbohydr. Res.* **1988**, *174*, 354.

(41) Nishida, Y.; Hori, H.; Ohrui, H.; Meguro, H. *J. Carbohydr. Chem.* **1988**, *7*, 239.

(42) Impey, R. W.; Madden, P. A.; McDonald, I. R. *J. Phys. Chem.* **1983**, *87*, 5071.

(43) Gonzalez-Outeirino, J.; Kirschner, K. N.; Thobhani, S.; Woods, R. J. *Can. J. Chem.* **2006**, *84*, 569.

(44) Kirschner, K. N.; Woods, R. J. *Proc. Natl. Acad. Sci. U.S.* **2001**, *98*, 10541.

(45) (a) Naidoo, K. J.; Chen, Y.-J. *Mol. Phys.* **2003**, *101*, 2687. (b) Chen, Y.-J.; Naidoo, K. J. *J. Phys. Chem. B* **2003**, *107*, 9558.

(46) Rockwell, G. D.; Grindley, T. B. *J. Am. Chem. Soc.* **1998**, *120*, 10953.

(47) Naidoo, K. J.; Kuttel, M. M. *J. Comput. Chem.* **2001**, *22*, 445.

JP8067409